


Geophysical Research Letters[®]

RESEARCH LETTER

10.1029/2024GL108583

Deciphering Controls of Pore-Pressure Evolution on Sediment Bed Erosion by Debris Flows

Hongchao Zheng^{1,2} , Xinli Hu¹, Zhenming Shi², Danyi Shen², and Tjalling De Haas³

¹Faculty of Engineering, China University of Geosciences (Wuhan), Wuhan, China, ²Department of Geotechnical Engineering, College of Civil Engineering, Tongji University, Shanghai, China, ³Department of Physical Geography, Faculty of Geosciences, Utrecht University, Utrecht, The Netherlands

Key Points:

- Propensity for pore pressure evolution of bed sediments during debris-flow erosion is evaluated by a Deborah number
- Significant pore pressure and accompanying intense erosion occur for wet bed sediments with undrained behavior
- Enhanced pore pressure of wet bed sediments reduces flow basal friction, increasing flow mobility and runout

Supporting Information:

Supporting Information may be found in the online version of this article.

Correspondence to:

X. Hu,
huxinli@cug.edu.cn

Citation:

Zheng, H., Hu, X., Shi, Z., Shen, D., & De Haas, T. (2024). Deciphering controls of pore-pressure evolution on sediment bed erosion by debris flows. *Geophysical Research Letters*, 51, e2024GL108583. <https://doi.org/10.1029/2024GL108583>

Received 29 JAN 2024

Accepted 27 FEB 2024

Author Contributions:

Conceptualization: Hongchao Zheng
Data curation: Danyi Shen, Tjalling De Haas

Formal analysis: Hongchao Zheng, Xinli Hu

Funding acquisition: Hongchao Zheng, Zhenming Shi

Investigation: Xinli Hu, Danyi Shen

Methodology: Hongchao Zheng, Xinli Hu

Project administration:

Hongchao Zheng, Zhenming Shi

Resources: Xinli Hu, Zhenming Shi

Supervision: Zhenming Shi, Tjalling De Haas

Abstract Pore-fluid pressure (PP) plays an important role in bed erosion, but the mechanisms that control PP evolution and the resulting feedbacks on flow dynamics are unclear. Here, we develop a general formulation, allowing quantification of the propensity for PP evolution of saturated and unsaturated bed sediments. We conduct erosion experiments by systematically varying grain composition and water content of beds, for investigating effects of PP evolution on flow erosion. With increasing water content, PP shows a slight rise in deforming beds with drained behavior but significant larger rise in undrained beds. Regardless of bed composition, the erosion rate of beds presents a synchronous change tendency with PP evolution due to the loss in basal friction. PP instigates positive feedback that induces a remarkable gain of flow velocity and momentum on wet beds with undrained behavior. Our results help explain observations of volume growth and long run out of debris flows.

Plain Language Summary Debris flows are common geophysical flows consisting of debris grains and muddy water. Debris flows can grow significantly in volume and mobility as they pick up loose sediment from gully bed and banks. The destructive potential of debris flows increases with increasing flow volume and run out. This brings about great challenges for effective early warning of debris flows, design of prevention measures and mapping of hazard zones related to human settlements. It is commonly believed that flow momentum is consumed by carrying static bed sediments. However, flows can gain momentum by overriding wet bed sediments. This can be explained by pore-pressure generation as debris flows move across wet beds. The increase of measured pore-fluid pressure is limited for beds with a low water content, but substantial for beds with a higher water content, which strongly affects the erosion rates of bed sediments. Flow velocity and momentum on wet beds are observed to increase significantly but slightly for dryer beds as a result of the pore-pressure feedback. These findings indicate that the debris composition of the catchment, the water content of bed sediment and the pore-pressure development should be evaluated when making predictions on debris-flow hazard.

1. Introduction

Debris flows, composed of debris grains and interstitial slurry, are among the most destructive and dangerous mass movements in mountainous regions worldwide (Dietrich & Krautblatter, 2019; Iverson, 1997). Debris flows are frequently triggered by extreme rainstorms (Bollschweiler & Stoffel, 2010; Graber et al., 2023), cliff failures (Rengers et al., 2020; Stoffel et al., 2014) and permafrost degradation (Damm & Felderer, 2013; Sovilla et al., 2006).

Researchers have long recognized that debris flows can significantly increase their volume by bed erosion or channel bank collapse during transport through a drainage network (e.g., Pierson, 1980; Wang et al., 2003; Stock & Dietrich, 2003; Breien et al., 2008; Santi et al., 2008; Guthrie et al., 2010; Schürch et al., 2011; Theule et al., 2015; Simoni et al., 2020; De Haas et al., 2022). Debris flows can inundate habitats and block rivers, possibly resulting in catastrophic dam-break floods—especially when they grow in volume by bulking (Dong et al., 2011; Jakob et al., 2005; Liu et al., 2014). The mapping of hazard zones and design of prevention countermeasures depend on debris-flow runout and volume (Frank et al., 2017; Zheng et al., 2022). In addition, the spatio-temporal evolution of landscapes is largely affected by debris-flow erosion and sediment deposition in large fan systems (De Haas et al., 2018; Hungr et al., 2005). It is therefore of importance to understand and take into account erosion mechanisms of debris flows (Iverson, 2012).

© 2024. The Authors.

This is an open access article under the terms of the [Creative Commons Attribution License](https://creativecommons.org/licenses/by/4.0/), which permits use, distribution and reproduction in any medium, provided the original work is properly cited.

Debris-flow erosion is a complex process related to the interaction between the overlying flow and sediment bed. The shear stresses induced by basal friction and collisional stresses generated by coarse particles are generally regarded as the driving mechanism for bed erosion (De Haas & van Woerkom, 2016; Hsu et al., 2014; Zheng et al., 2021). Pore-fluid pressure (PP) at the interface arising from the flow transmission and shear contraction of the bed strongly regulates the erosion and mobility of debris flows by counteracting the intergranular friction and grain collision (Kaitna et al., 2016). The pioneer experimental work conducted by Iverson et al. (2011) indicates that significant erosion occurs when a high PP develops in wet beds, whereas PP development and erosion are negligible in dry beds. Similarly, high erosion rates where significant PP develops have subsequently been observed in field measurements and laboratory experiments of debris flows (McCoy et al., 2012; Roelofs et al., 2023). However, the effect of PP evolution on bed erosion is commonly explained on the basis of saturated soil mechanics (Iverson, 2012). In reality, however, channel beds are generally initially unsaturated and transitioning into saturated as the flow overrides the bed (Berti & Simoni, 2005; Song & Choi, 2021).

The underlying mechanisms that control pore-pressure evolution in saturated and unsaturated beds are largely unknown. In particular, the basic physics on how PP evolves in response to bed deformation by debris flows, the resulting feedback effects, and how this affects bed erosion still remains unclear.

Here we propose a general formulation for PP evolution in sediment beds overridden by debris flows and aim to address the following fundamental questions.

- How do water content and grain composition of the bed control PP development?
- Is there a critical water content above which a significantly increased PP response causes enhanced bed erosion?
- Can PP development within a sediment bed instigate erosion and increase flow mobility?

We develop a theoretical model for PP development in saturated and unsaturated beds during flow erosion, which allows quantification of the propensity for pore-fluid pressurization of bed sediments by a Deborah number. A series of erosion experiments under closely controlled conditions are conducted to interpret the mechanisms that control PP development on basis of shearing bed behavior, and to analyze the effects of PP feedback on bed erosion and flow characteristics.

2. Propensity for Pore-Pressure Generation in Sediment Beds Overridden by Debris Flows

PP within bed sediment rapidly changes when overridden by debris flow. According to mass conservation and Darcy laws, a diffusion equation describing the PP evolution in response to overlying flow is derived (Iverson, 2012; Zheng et al., 2023)

$$\frac{dp}{dt} = \nabla \cdot \frac{k}{C\mu} \nabla p + \frac{d\sigma}{dt} - \frac{\dot{\gamma} \tan \varphi}{C} \quad (1)$$

where p is the pore pressure and σ is the total normal stress of the overriding flow; k (m^2) is the bed permeability and μ (Pa s) is the fluid viscosity; t (s) is the time and $\dot{\gamma}$ (s^{-1}) is the bed shear rate; C (m^2/N) is the drained compressibility of the bulk bed material; φ is a dilatancy angle that characterizes the propensity of the bed to dilate ($\varphi > 0$) or contract ($\varphi < 0$). Bed sediment is naturally loose and unconsolidated and thus shear dilation with $p < 0$ is not considered herein. This formulation indicates that PP evolution depends on the diffusivity (second term) and the bulk compression by flow weight (third term) as well as shear-induced bed contraction (fourth term).

A non-dimensional analysis is conducted to assess the relative importance of different terms in Equation 1. The characteristic magnitudes of the variables are expressed as $p = \hat{p}/C$, $t = \hat{t}/t_0$, $\sigma = \hat{\sigma}/C$, $\dot{\gamma} = \hat{\dot{\gamma}}/t_0$, where the $\hat{}$ symbol denotes non-dimensional variables, and t_0 is a timescale factor. The first divergence in the diffusivity term signifying particle-size movement is scaled by characteristic particle diameter d_g^{-1} and the second divergence representing the PP diffusion dimension is scaled by $l = \sqrt{D t_0}$, where $D = k/(C\mu)$ is the PP diffusion coefficient, and $t_0 = d_g/u_0$ is the timescale with respect to particle deformation, u_0 is the bed-grain velocity.

Substituting these dimensionless variables to Equation 1 yields

$$\frac{d\hat{p}}{d\hat{t}} = \frac{D}{lu_0} \hat{v}_1 (\hat{v}_2 \hat{p}) + \frac{d\hat{\sigma}}{d\hat{t}} - \hat{\gamma} \tan \varphi \quad (2)$$

The coefficients of the second term in Equation 2 can be presented as:

$$\frac{D}{lu_0} = \sqrt{\text{De}_d^{-1}} \quad (3)$$

The Deborah number, $\text{De}_d = t_d/t_0$, is used to characterize the relative magnitude of a relaxation timescale and a characteristic process timescale (Osswald, 1998). Here, the relaxation timescale, $t_d = d_g^2/D$, is the timescale for PP diffusion across a single grain and the characteristic process timescale, t_0 , is the timescale of grain deformation (Zheng et al., 2023). De_d signifies PP evolution propensity of a single grain eroded by debris flow.

In the analysis, we aim to investigate the effects of shearing behavior of the beds with a specific thickness on the PP evolution. Analogously, it is necessary to assign another Deborah number, $\text{De}_\zeta = t_\zeta/t_e$, which shows the relative magnitude between $t_\zeta = h^2/D$, the timescale of PP diffusion over a saturated zone, and t_e , the timescale of bed erosion. h is the thickness of saturated bed zone.

We consider a debris flow to transport across an erodible bed overlying a fixed bed with a non-flux boundary (Figure S1 in Supporting Information S1). For an initially unsaturated bed, $h = h_i$, the depth of upper saturated zone due to flow infiltration during the timescale t_e for bed erosion. Based on the Green–Ampt model (Chen & Young, 2006; Green & Ampt, 1911), h_i is approximated to $h_i = f(\theta) = \frac{K t_e}{\Delta\theta}$ (Appendix in Supporting Information S1), where $K = \frac{k\rho_f g}{\mu}$ is the hydraulic conductivity of saturated bed above the wetting front. ρ_f is the mass density of the pore fluid and g is the gravitational acceleration. θ_s and θ_i are the volumetric water content for saturated and initially unsaturated bed sediments, respectively. $\Delta\theta = \theta_s - \theta_i$ is the water-content difference between these two beds. Thus, De_ζ of the unsaturated bed is expressed as

$$\text{De}_\zeta = \frac{K^2 t_e}{\Delta\theta^2 D} \quad (4)$$

The maximum infiltration depth h_i equals the erodible bed thickness H . This situation occurs for an initially saturated bed or during transition from unsaturated to saturated bed during erosion. De_ζ of a saturated bed yields to $\text{De}_\zeta = \frac{H^2}{D t_e}$.

The propensity of PP evolution depends on the diffusive dissipation of pore pressure relative to the effects of shearing and compression of the bed indicated by Equation 2. With $\text{De}_\zeta < 1$, PP dissipation is effective and can easily diffuse from the shearing bed to the boundaries within the erosion timescale, exhibiting drained behavior. In contrast, with $\text{De}_\zeta > 1$, PP dissipation is relatively limited and the diffusion front originating along the shearing layer does not reach the boundaries, leading to undrained behavior (Figure S1 in Supporting Information S1). PP with regard to drained behavior generally has a lower magnitude than the value of undrained beds under the same loading condition.

De_ζ in Equation 4 motivates measurements of PP evolution during flow erosion by altering water content and permeability of the beds. A chief aim of our experiments was to decipher controls of the PP evolution on the bed erosion by systematically varying De_ζ , and simultaneously assess resulting feedback on changes in flow velocity and momentum. This is different from previous bed erosion studies (Iverson et al., 2011; McCoy et al., 2012; Roelofs et al., 2023).

3. Materials and Methods

We conducted 20 experiments in which water-saturated 0.055 m³ debris flows were released within 0.5 s by opening a gate and then flowed over unsaturated beds in a 4 m long, 0.3 m wide flume (Figure S2 in Supporting Information S1). The approximately tabular sediment beds averaged 0.08 m in thickness and covered the straight-slope flume bed ($\alpha = 27^\circ$) from $x = 0.9$ –3.6 m, where $x = 0$ represents the location of the opening gate.

The grain composition and initial water content θ_i of the movable bed were the pivotal variables we varied. Three grain compositions termed fine-grained, uniformly graded and coarse-grained sediments (Figure S3 in Supporting Information S1) were derived by the interpretation of historical data from 1,728 debris flows originating from different-lithology basins in the Northwestern Alps (Tiranti et al., 2008). The magnitude of saturated hydraulic conductivity K measured from constant-head permeameter tests (Shi et al., 2018) ranged from 10^{-6} m/s to 10^{-3} m/s and diffusion coefficient D obtained by consolidation tests (Major, 2000) varied within 10^{-6} – 10^{-4} m²/s for different bed sediments with the same dry density to those prepared in erosion experiments (Figure S3 in Supporting Information S1). The released flows consisted of the uniformly graded debris mixture and had a bulk density of 1,800 kg/m³.

The initial volumetric water content θ_i of the bed was determined by controlling water quantity during debris mixing. Bed material lying on the flume bottom had dry densities of 1,700 kg/m³. θ_i of fine-grained and uniformly graded debris were varied in the range of 0–0.25 prior to debris-flow release, whereas those for coarse-grained debris varied from 0 to 0.20 due to its poor water retention capacity. The erosion experiments with $\theta_i = 0.15$ were repeated twice for these three beds to consider the effects of natural variability.

Three video cameras (GZ-R10BAC, JVC, frame rate of 25 Hz), above the flume were used to observe the movement of debris flows. A high-speed camera (i-SPEED7, iX Cameras, frame rate of 200 Hz) in the cross-stream direction recorded the erosion process. A 3D laser scanner (ScanStation P40, Leica, measurement accuracy 1.2 mm + 10 ppm) was used to acquire bed thicknesses before and after flow release. At $x = 1.8$ m we deployed arrays of electronic sensors to measure the flow level h and pore pressure p with a sample frequency of 500 Hz. The flow surface level was monitored by an ultrasonic sensor (T30U, Banner, measurement accuracy 1.0 mm). Details with respect to sensor calibrations, uncertainty analysis, bed preparation and data processing methods are described in Zheng et al. (2021).

For evaluating the mass and momentum of debris flows in the process of erosion on different beds, we quantify average flow-front velocity and flow volume over the $x = 0.9$ – 3.6 m reach. The flow-front velocity was measured by recorded snapshots and a steel tape fixed on the flume sidewall. The erosion volume of bed sediment was calculated by using gridded digital elevation models (DEM) before and after flow passage and the post-erosion flow volume was the sum of the initial flow volume and erosion volume. For distinguishing any significant change from noise, the DEM differences of bed surface were filtered by a minimum level of detection threshold, which was estimated to the squared sum of the standard deviations of DEM errors (Lane et al., 2003; Wheaton et al., 2010).

4. Results

4.1. Pore-Pressure Evolution During Flow Erosion

Following opening of the gate, debris flows rapidly accelerated when they moved to $x \approx 1.0$ m as a result of the dam-break initial conditions. Downstream sediment beds strongly affected flow behavior. Debris flows that encountered the coarse-grained beds appeared to behave almost explosively as their maximum flow depths exceeded 15 cm (Figure 1 and Figure S4 in Supporting Information S1). In contrast, debris flows that traveled across fine-grained beds had a maximum flow depth of less than 10 cm, which were slightly smaller than those for the uniformly graded beds with an approximate flow depth of 11 cm.

PP beneath the bed rapidly changed following the arrival of the flow front. A positive correlation existed between PP and bed water content irrespective of the bed materials. PP developed in the coarse-grained beds was higher than those in fine-grained and uniformly graded beds with the same water content. Concomitant obvious fluctuations occurred for PP generated within wet beds with a large water content (Figures 1f, 1h and 1i), indicating severe erosion close to the sensor.

4.2. Bed Erosion Regulated by Pore Pressure

De_c increased with increase of water content θ_i regardless of bed sediments because the PP diffusion timescale over a saturated zone was enlarged (Figure 2a). Drained behavior ($De_c < 1$) tended to transition to undrained behavior ($De_c > 1$) for the unsaturated uniformly graded and coarse-grained beds with increasing θ_i . For $\theta_i = 0.20$, the infiltration depth ($h_i = \frac{K_s}{\Delta\theta}$) of coarse-grained beds within the erosion timescale was several centimeters, the

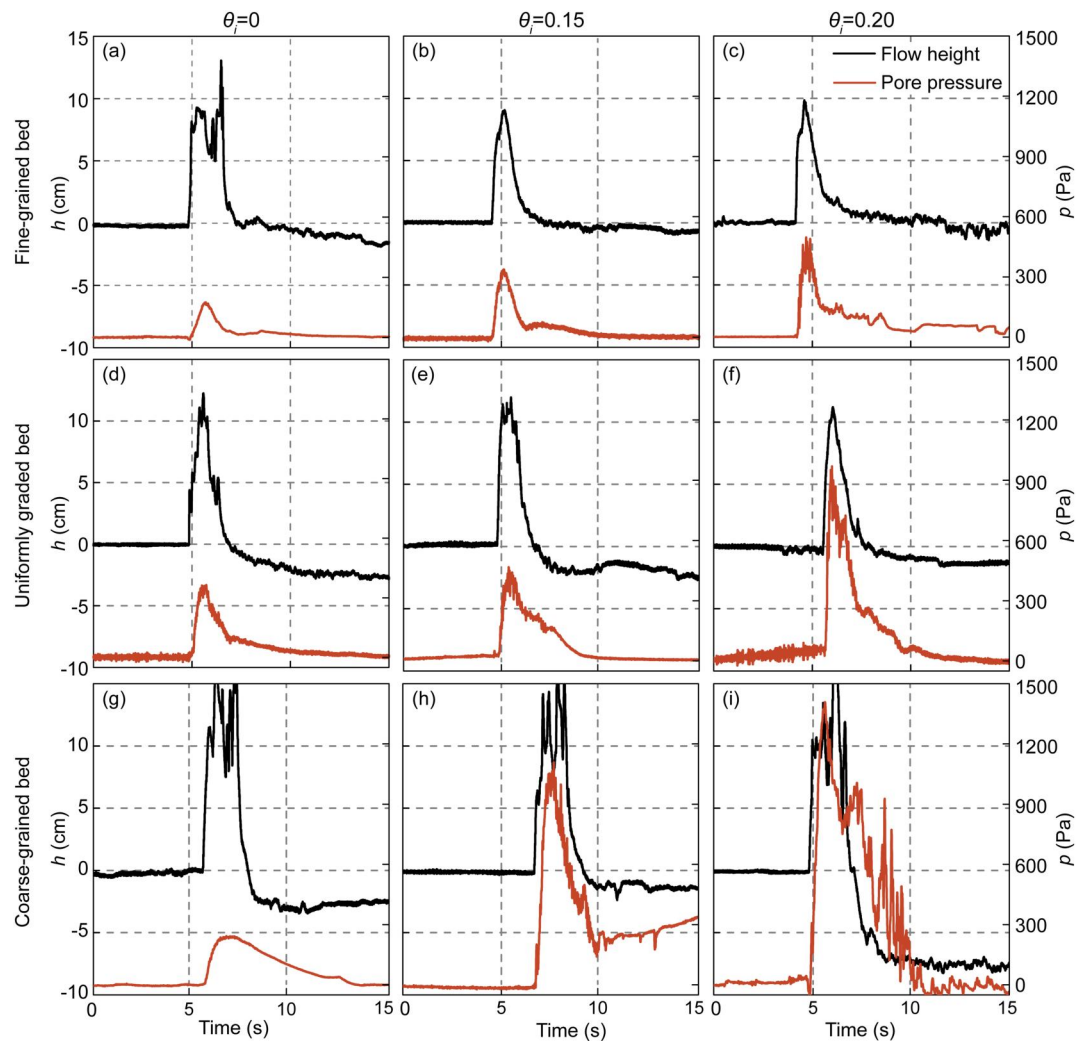


Figure 1. Time-series data monitored at $x = 1.8$ m in nine experiments with increasing bed water content. Sensor measurements of flow surface level $h(t)$ (black line) and basal pore pressure $p(t)$ (red line) for fine-grained (a–c), uniformly graded (d–f) and coarse-grained (g–i) sediment beds. A negative flow surface level indicates the bed sediment was eroded by the overriding flow.

same order of magnitude as the bed thickness, contributing to the increases in length (infiltration depth) and timescale of PP diffusion (Equation 4). However, the flow infiltration into unsaturated fine-grained beds had a magnitude of less than a millimeter due to a low hydraulic conductivity ($K = 2.3 \times 10^{-6}$ m/s). As a result, drained behavior only occurred in fine-grained beds.

The growth of the maximum pore pressure p_m versus water content was slight for bed sediments having drained behavior (Figure 2b). p_m varied in the range of 173–485 Pa and showed an approximately linear relationship with water content for different beds. In such circumstances, shearing beds were dominated by drained behavior. Pore-fluid pressurization rate $\frac{dp}{dt}$ presents a negative correlation with the PP diffusion term indicated by Equation 2 and water content difference $\Delta\theta$ is located in the numerator of the diffusion term, resulting in a linear tendency for PP generation. A robust growth in p_m larger than 900 Pa occurred in beds that transitioned from drained to undrained behavior with increasing water content. Pore fluid within bed sediment was pressurized by flow loading and shear contraction (Equation 2) and PP diffusion was relatively weak, causing a high PP. The critical water content θ_c corresponding to a significant increase in PP for uniformly graded and coarse-grained beds were close to 0.20 and 0.15, respectively.

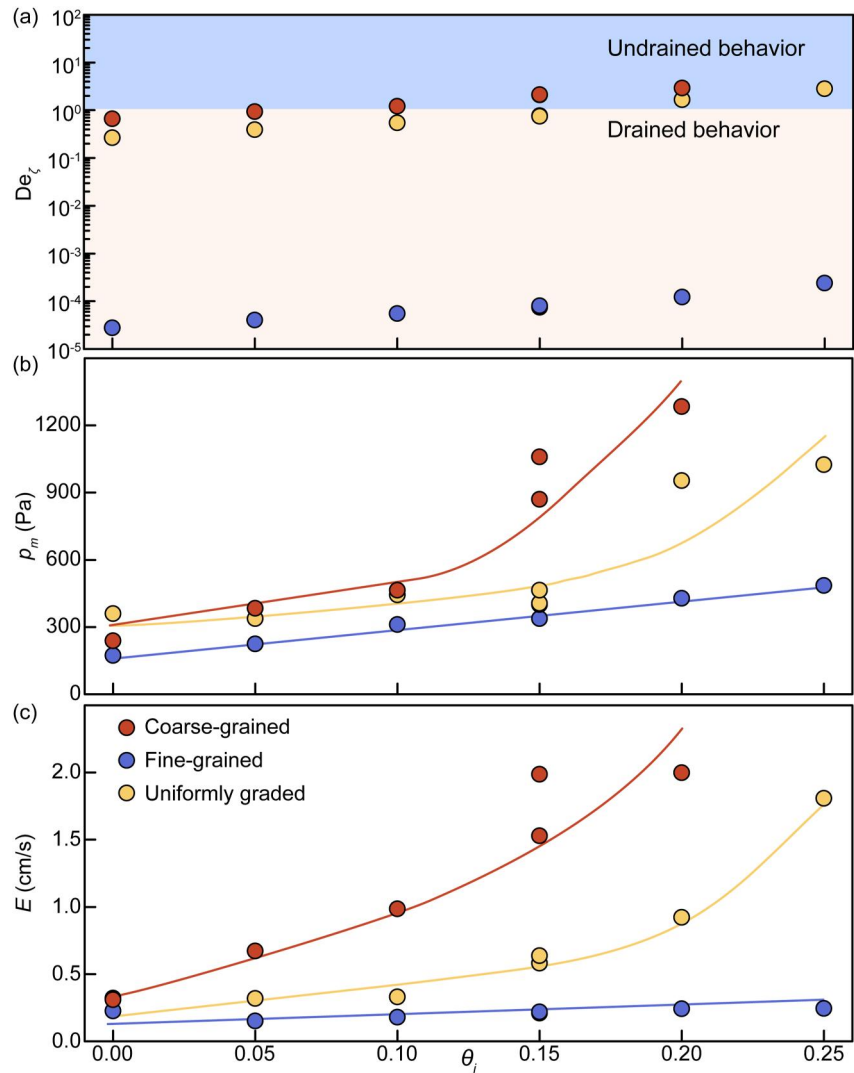


Figure 2. Deborah number De_z , maximum pore pressure p_m and erosion rate E of fine-grained, uniformly graded and coarse-grained sediment beds with increasing initial water content θ_i . Panel (a) shows how sediment beds present drained behavior with $De_z < 1$ and transition to undrained behavior with $De_z > 1$ inferred from Equation 2. Solid lines in panels (b) and (c) denote linear fitting for fine-grained beds and segmental fitting using linear and quadratic functions for coarse-grain and uniformly graded beds. Erosion rate E is calculated by the erosion volume V_e divided by the corresponding erosion time t_e (see Table S1 in Supporting Information S1).

The mean erosion rate E of beds showed a positive correlation with water content (Figure 2c). Based on a limit equilibrium analysis, the calculated erosion rate E_c is proportional to the difference between the shear stress exerted by the overlying flow τ_f and bed frictional stress τ_b (Iverson, 2012), which is expressed as

$$E_c = \frac{\tau_f - \tau_b}{\rho V_f} = \frac{\rho g h \sin \alpha - (\rho g h \cos \alpha - p) \tan \varphi_b}{\rho V_f} \quad (5)$$

where V_f is the flow velocity, α and φ_b are the flume angle (27°) and bed friction angle, respectively. Because the flow front had an approximately steady velocity, τ_f approaches the stress generated by the downslope gravity $f_g = \rho g h \sin \alpha$. p played an important role in the erosion rate in Equation 5, whereas the variations of h and V_f were relatively limited for flows on a specified sediment bed. As a consequence, E presented a synchronous change tendency with p_m by comparing Figures 2b and 2c. The mean erosion rates of fine-grained beds were close to 2.0 mm/s and fine-grained sediment was progressively scoured grain by grain on the bed surface (Figure S4 in

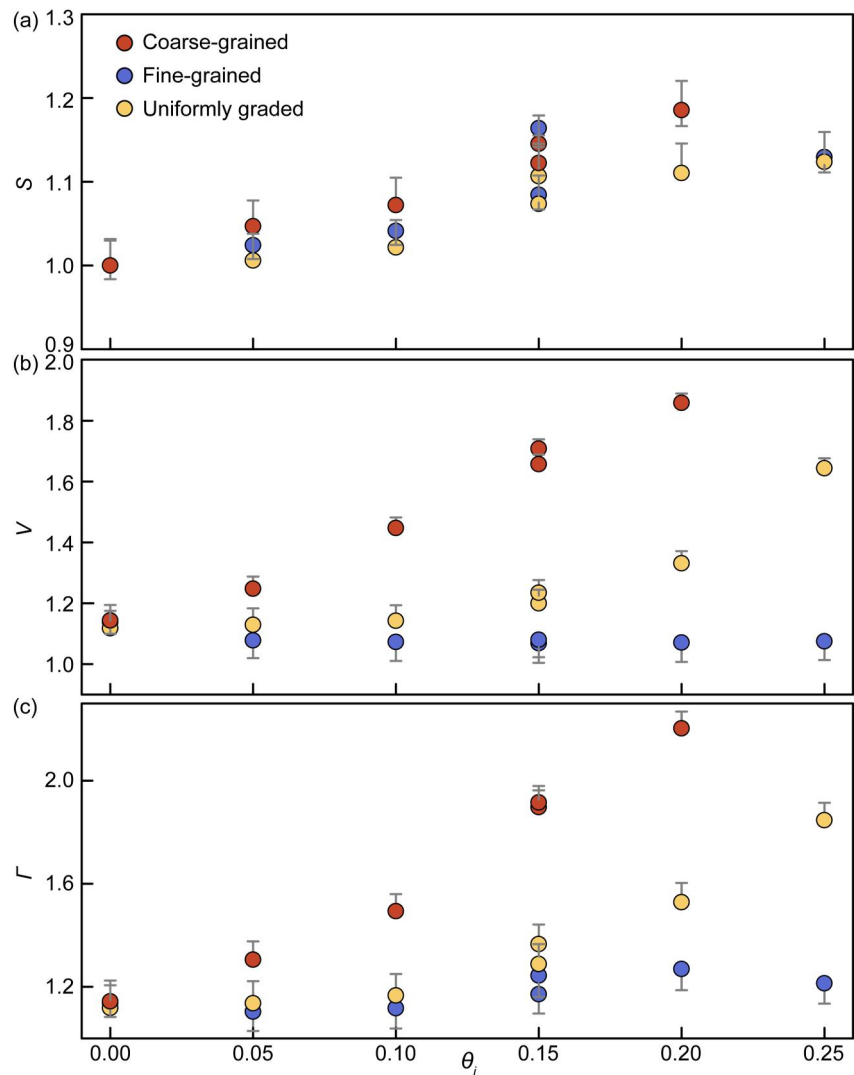


Figure 3. Post-erosion flow parameters as a function of bed water content for different beds: (a) normalized flow-front velocities S ; (b) normalized flow volumes V ; (c) normalized momentum growths Γ over the sediment beds. Error bars for S , V and Γ represent accumulated measurement uncertainties in erosion time and volume. The error bars of all data points are showed with one side, considering the top error is equal to the bottom error.

Supporting Information S1). In contrast, the values for uniformly graded and coarse-grained beds with undrained behavior had a magnitude of 1.0 cm/s due to a high PP. These beds were entrained by en masse entrainment of a layer with a depth of several centimeters. For instance, for a coarse-grained bed with $\theta_i = 0.20$ ($p_m = 1,284$ Pa, $h = 0.15$ m, $\tan\phi_b = 0.88$), E_c was calculated to be 3.2 cm/s, which was in accordance with the measured mean value. In addition, the upper limit of the volumetric concentration of the flow (Takahashi, 2007) was not achieved during bed erosion considering debris deposition was observed on the bed surface.

4.3. Measured Mass and Momentum Changes

Flow-front velocities V_f on fine-grained beds increased from 2.67 to 3.02 m/s with increasing water content, which were larger than corresponding values on uniformly graded and coarse-grained beds. This is because fine-grained sediments have the smallest friction angle. We compare observations of flow-front velocity, erosion volume and momentum gain by normalizing the variables following the approach of Iverson et al. (2011). Normalized velocities S defined as V_f divided by reference velocity on a dry bed with $\theta_i = 0$ generally increased with θ_i (Figure 3a). The variation tendency of S was approximately consistent for different beds.

Debris flows that flowed over wet beds also entrained more sediment and showed longer run-out distances than flows that moved across dryer beds (Table S1 in Supporting Information S1). Normalized post-erosion flow volumes V defined as total flow volume divided by released flow volume exceeded one in each experiment and increased consistently with θ_i (Figure 3b). Moreover, coarse-grained and uniformly graded beds had a larger gain in V than those for fine-grained beds due to the low erosion rates of the latter (Figure 2c).

A normalized momentum growth factor defined as $\Gamma = VS$ was adopted to quantitatively evaluate the effects of bed erosion on flow momentum. $\Gamma > 1$ applicable for all wet beds indicates a momentum increase compared to the reference values obtained by experiments with dry beds (Figure 3c). $\Gamma < 1.4$ overall existed for beds with drained behaviors, whereas $\Gamma > 1.5$ was applicable for beds with undrained behavior. Particularly, for flow on the wettest coarse-grained bed, flow-momentum increased by a factor 2 due to PP feedback in response to the bed erosion.

The propensity for flow momentum growth is elucidated by different PP evolutions. When flows started to entrain the beds with $De_\zeta > 1$ (undrained conditions), PP rose to magnitudes sufficient to substantially liquefy the sediment beds with a liquefaction ratio (p_m divided by flow normal stress) $L > 0.7$. This high PP was sustained when most of bed sediment was eroded (Figures 1f, 1h and 1i). Despite the fact that momentum is transferred from the overlying flow to the sediment bed with a negligible velocity, flow momentum grew considering the reduction in basal friction resistance, which exceeded 70%. In contrast, a low PP persisted and $L < 0.4$ during flow interaction with relatively dryer beds ($De_\zeta < 1$) and thus the momentum growth was relatively limited.

5. Discussion

5.1. Critical Water Content of Bed Sediments With Undrained Behavior

The growths of measured PP and erosion rate are slight for beds with water content $\theta_i < \theta_c$ whereas, dramatic growths exist for beds with $\theta_i > \theta_c$, indicating the beds present undrained behavior. These phenomena are in accordance with experimental observations by Roelofs et al. (2023) and Iverson et al. (2011) as well as in-field measurements by McCoy et al. (2012). PP evolution and momentum growth measured by Iverson et al. (2011) are reasonably elucidated by Deborah number derived by our theoretical model (Figure S5 in Supporting Information S1).

Critical water content θ_c corresponding to a significant increase in PP during flow erosion are collected from the tested debris flows presented here and related data from literature (Figure 4). θ_c are negatively linearly correlated with the hydraulic conductivity K of bed sediments. For a given De_ζ that characterizes bed transition from drained to undrained behavior, K is proportional to the water content difference $\Delta\theta$ and thus presents a linear correlation with θ_c indicated by Equation 4. This hydraulic conductivity of beds in the regression line has the same magnitude as those of natural channel sediments with silty sands of 10^{-6} m/s to gravel soils of 10^{-2} m/s (Tiranti et al., 2008). As a consequence, the propensity for PP evolution in natural gully beds can be evaluated before debris-flow initiation when hydraulic conductivity and initial water content of sediment are acquired.

For an initially saturated bed or an initially unsaturated bed transitioning to a saturated bed during flow erosion, De_ζ has a larger magnitude than the values for unsaturated beds. As a result, a higher PP occurs when saturated beds are overridden by debris flows as inferred from field data (McCoy et al., 2012). For saturated bed sediment, the PP diffusion timescale ($t_\zeta = H^2/D$) is reduced with increasing permeability k , indicating PP is prone to dissipation during erosion. As a consequence, the propensity for pore fluid pressurization diminishes. In contrast, this propensity is enhanced with increasing permeability and water content θ_i of unsaturated bed sediment, which is coherent with observations of natural debris flows at Sedgwick Reserve (Gabet & Mudd, 2006). This is due to the increases in the PP diffusion length ($h_i = \frac{Kt_\zeta}{\Delta\theta}$) and diffusion timescale, and explains why the maximum PP occurs in the coarse-grained sediment in our experiments with unsaturated beds, while PP would be highest in low-permeability beds under saturated conditions. A detailed comparison of propensity for PP evolution within saturated and unsaturated beds is given in Zheng et al. (2023).

5.2. Effects of Pore-Pressure Feedback on Bed Erosion and Flow Characteristics

The erosion rate is significantly faster for wet beds with $\theta_i \geq \theta_c$ compared to rates for relatively dryer beds (Figure 2c). This trend was also observed in channel bed erosion by debris flows measured in Chalk Cliffs, USA (McCoy et al., 2012), and the Illgraben, Switzerland (De Haas et al., 2022), large flume tests

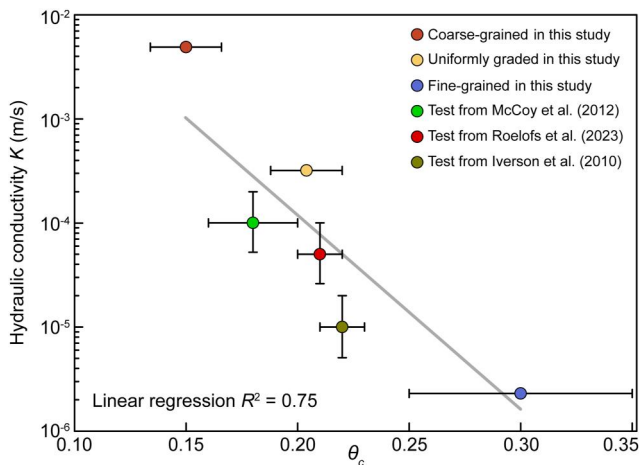


Figure 4. Critical water content θ_c versus hydraulic conductivity K . Data from McCoy et al. (2012) was measured at the Chalk Cliffs debris-flow monitoring station and channel sediment consisted of gravel, sand, silt and clay. Data from Iverson et al. (2011) was acquired by large-scale flume tests with the beds composed of gravel, sand and mud. Data from Roelofs et al. (2023) was obtained by laboratory tests with the beds composed of gravel and sand. Critical water content of fine-grained beds in our tests was estimated to vary from initial water content $\theta_i = 0.25$ to saturated water content. R^2 is the determination coefficient.

in the USGS flume (Iverson et al., 2011) as well as in laboratory tests by Roelofs et al. (2023). Pore fluid is dramatically pressurized in comparison to PP diffusion (Equation 2) when flows deform beds with undrained behavior as a result of contraction. The effective stress is counteracted by PP and bed frictional resistance is reduced (Equation 5). As a result, the relation between mean erosion rate and water content is the same to the relation of PP and water content (Figures 2b and 2c). This difference in PP evolution explains why coarse-grained and uniformly graded beds with high friction angles generally have a larger mean erosion rate than fine-grained beds with low friction angle at the same water content.

The bed erosion can be associated with PP fluctuations. High PP fluctuations occur for debris flows measured in vertically rotating drums due to the collisions of coarse grains during flow (Kaitna et al., 2016). Indeed, PP fluctuations disappear for debris flows in deposition from consolidation tests (Kaitna et al., 2016; Major, 2000). High PP fluctuations can also be induced by intense erosion of bed sediment as indicated by our tests (Figure 1). This phenomenon is also observed in field measurements at Chalk Cliffs wherein large-magnitude, high frequency PP fluctuations are obtained in near-surface bed sediments (McCoy et al., 2012). Irrespective of the sources of the PP fluctuations, concomitant fluctuations in Coulomb frictional resistance instigate bed erosion.

Our results show that the PP feedback on the erosion process significantly affects flow characteristics. Due to a low erosion rate, flows depths on fine-grained beds were lower than those on coarse-grained and uniformly

graded beds (Figure 1). The enhanced PP persists in the process of flow erosion and promotes progressive erosion of the bed (Equation 5), resulting into increases in flow velocity, volume and momentum. As a result, compared to flows on dry beds, flow velocity and momentum on wet beds observably increase (Figure 3). This phenomenon can explain debris-flow volume bulking and long run-out distances, where flows gain mass and momentum when entraining the channel bed (Pierson, 1980; Stoffel et al., 2014). Furthermore, it offers implications for clarifying mechanisms that debris flows initiate in the same basins but exhibit significant differences in transportation distance and deposit morphology without the influence of torrent topography (De Haas et al., 2018).

6. Conclusions

We developed a theoretical model applicable for saturated and unsaturated bed sediments containing clay, sand and gravel and evaluated the state of the bed (drained or undrained) by a Deborah number during debris-flow erosion. We conducted a series of erosion experiments for investigating effects of PP evolution on bed erosion and resulting feedbacks on flow characteristics. Our main findings are.

1. The bed sediments overridden by debris flows can present drained or undrained behavior. This propensity is quantitatively evaluated by a Deborah number De_ζ defined as the timescale ratio of PP diffusion to bed erosion: deforming beds with $De_\zeta < 1$ and $De_\zeta > 1$ are dominated by drained and undrained behaviors, respectively.
2. The growth of measured PP versus water content is slight and linear for beds presenting drained behavior, whereas an enhanced growth in PP occurred for beds transitioning to undrained behavior. The mean erosion rate is strongly related to PP evolution because bed strength is strongly reduced by enhanced PP.
3. The PP evolution of deforming beds has positive feedback on debris-flow characteristics. Irrespective of the grain composition, flow velocity and momentum progressively increase with increasing initial bed water content. Particularly, momentum growth (close to 2 times) is substantial for wet bed sediments with undrained behavior due to the frictional resistance reduced by persisted high PP.

Data Availability Statement

The measured flow surface level and basal pore pressure at $x = 1.8$ m are available at <https://doi.org/10.5281/zenodo.10213024>.

Acknowledgments

We acknowledge funding from the Natural Science Foundation of China (No. 42307196) and National Key Research and Development Program of China (No. 2023YFC3007001). Constructive reviews by the editors and two anonymous reviewer helped to improve the manuscript and are gratefully acknowledged.

References

- Berti, M., & Simoni, A. (2005). Experimental evidences and numerical modelling of debris flow initiated by channel runoff. *Landslides*, 2(3), 171–182. <https://doi.org/10.1007/s10346-005-0062-4>
- Bollschweiler, M., & Stoffel, M. (2010). Changes and trends in debris-flow frequency since AD 1850: Results from the Swiss Alps. *The Holocene*, 20(6), 907–916. <https://doi.org/10.1177/0959683610365942>
- Breien, H., De Blasio, F., Elverhøi, A., & Høeg, K. (2008). Erosion and morphology of a debris flow caused by a glacial lake outburst flood, western Norway. *Landslides*, 5(3), 271–280. <https://doi.org/10.1007/s10346-008-0118-3>
- Chen, L., & Young, M. (2006). Green-Ampt infiltration model for sloping surfaces. *Water Resources Research*, 42(7), W07420. <https://doi.org/10.1029/2005wr004468>
- Damm, B., & Felderer, A. (2013). Impact of atmospheric warming on permafrost degradation and debris flow initiation: A case study from the eastern European Alps. *E&G Quaternary Science Journal*, 62(2), 136–149. <https://doi.org/10.3285/eg.62.2.05>
- De Haas, T., Densmore, A., Stoffel, M., Suwa, H., Imaizumi, F., Ballesteros-Cánovas, J., & Wasklewicz, T. (2018). Avulsions and the spatio-temporal evolution of debris-flow fans. *Earth-Science Reviews*, 177, 53–75. <https://doi.org/10.1016/j.earscirev.2017.11.007>
- De Haas, T., McArdell, B., Nijland, W., Åberg, A., Hirschberg, J., & Huguénin, P. (2022). Flow and bed conditions jointly control debris-flow erosion and bulking. *Geophysical Research Letters*, 49(10), e2021GL097611. <https://doi.org/10.1029/2021GL097611>
- De Haas, T., & van Woerkom, T. (2016). Bed scour by debris flows: Experimental investigation of effects of debris-flow composition. *Earth Surface Processes and Landforms*, 41(13), 1951–1966. <https://doi.org/10.1002/esp.3963>
- Dietrich, A., & Krautblatter, M. (2019). Deciphering controls for debris-flow erosion derived from a LiDAR-recorded extreme event and a calibrated numerical model (Roßbichelbach, Germany). *Earth Surface Processes and Landforms*, 44(6), 1346–1361. <https://doi.org/10.1002/esp.4578>
- Dong, J., Li, Y., Kuo, C., Sung, R., Li, M., Lee, C., et al. (2011). The formation and breach of a short-lived landslide dam at HsiaoLin village, Taiwan—Part I: Post-event reconstruction of dam geometry. *Engineering Geology*, 123(1–2), 40–59. <https://doi.org/10.1016/j.enggeo.2011.04.001>
- Frank, F., McArdell, B., Oggier, N., Baer, P., Christen, M., & Vieli, A. (2017). Debris-flow modeling at Meretschibach and Bondasca catchments, Switzerland: Sensitivity testing of field-data-based entrainment model. *Natural Hazards and Earth System Sciences*, 17(5), 801–815. <https://doi.org/10.5194/nhess-17-801-2017>
- Gabet, E., & Mudd, S. (2006). The mobilization of debris flows from shallow landslides. *Geomorphology*, 74(1–4), 207–218. <https://doi.org/10.1016/j.geomorph.2005.08.013>
- Graber, A., Thomas, M., & Kean, J. (2023). How long do runoff-generated debris-flow hazards persist after wildfire? *Geophysical Research Letters*, 50(19), e2023GL105101. <https://doi.org/10.1029/2023gl105101>
- Green, W., & Ampt, G. (1911). Studies on soil physics. *Journal of Agricultural Science*, 4(1), 1–24. <https://doi.org/10.1017/s0021859600001441>
- Guthrie, R., Hockin, A., Colquhoun, L., Nagy, T., Evans, S., & Ayles, C. (2010). An examination of controls on debris flow mobility: Evidence from coastal British Columbia. *Geomorphology*, 114(4), 601–613. <https://doi.org/10.1016/j.geomorph.2009.09.021>
- Hsu, L., Dietrich, W., & Sklar, L. (2014). Mean and fluctuating basal forces generated by granular flows: Laboratory observations in a large vertically rotating drum. *Journal of Geophysical Research: Earth Surface*, 119(6), 1283–1309. <https://doi.org/10.1002/2013jef003078>
- Hungr, O., McDougall, S., & Bovis, M. (2005). Entrainment of material by debris flows. In *Debris flow hazards and related phenomena* (pp. 135–158). Springer Berlin Heidelberg. https://doi.org/10.1007/3-540-27129-5_7
- Iverson, R. (1997). The physics of debris flows. *Reviews of Geophysics*, 35(3), 245–296. <https://doi.org/10.1029/97rg00426>
- Iverson, R. (2012). Elementary theory of bed-sediment entrainment by debris flows and avalanches. *Journal of Geophysical Research*, 117(F3), F03006. <https://doi.org/10.1029/2011jef002189>
- Iverson, R., Reid, M., Logan, M., LaHusen, R., Godt, J., & Griswold, J. (2011). Positive feedback and momentum growth during debris-flow entrainment of wet bed sediment. *Nature Geoscience*, 4(2), 116–121. <https://doi.org/10.1038/ngeo1040>
- Jakob, M., Hungr, O., & Jakob, D. (2005). In M. Jakob & O. Hungr (Eds.), *Debris-flow hazards and related phenomena* (Vol. 135–158). Springer.
- Kaitna, R., Palucis, M., Yohannes, B., Hill, K., & Dietrich, W. (2016). Effects of coarse grain size distribution and fine particle content on pore fluid pressure and shear behavior in experimental debris flows. *Journal of Geophysical Research: Earth Surface*, 121(2), 415–441. <https://doi.org/10.1002/2015jef003725>
- Lane, S., Westaway, R., & Hicks, D. (2003). Estimation of erosion and deposition volumes in a large, gravel-bed, braided river using synoptic remote sensing. *Earth Surface Processes and Landforms*, 28(3), 249–271. <https://doi.org/10.1002/esp.483>
- Liu, J., You, Y., Chen, X., Liu, J., & Chen, X. (2014). Characteristics and hazard prediction of large-scale debris flow of Xiaojia Gully in Yingxiu Town, Sichuan Province, China. *Engineering Geology*, 180, 55–67. <https://doi.org/10.1016/j.enggeo.2014.03.017>
- Major, J. (2000). Gravity-driven consolidation of granular slurries: Implications for debris-flow deposition and deposit characteristics. *Journal of Sedimentary Research*, 70, 64–83. <https://doi.org/10.1306/d4268b8f-2b26-11d7-8648000102c1865d>
- McCoy, S., Kean, J., Coe, J., Tucker, G., Staley, D., & Wasklewicz, T. (2012). Sediment entrainment by debris flows: In situ measurements from the headwaters of a steep catchment. *Journal of Geophysical Research*, 117(F3), F03016. <https://doi.org/10.1029/2011jef002278>
- Osswald, T. (1998). *Polymer processing fundamentals*. Hanser Gardner.
- Pierson, T. (1980). Erosion and deposition by debris flows at Mt. Thomas, North Canterbury, New Zealand. *Earth Surface Processes*, 5(3), 227–247. <https://doi.org/10.1002/esp.3760050302>
- Rengers, F., Kean, J., Reitman, N., Smith, J., Coe, J., & McGuire, L. (2020). The influence of frost weathering on debris flow sediment supply in an alpine basin. *Journal of Geophysical Research: Earth Surface*, 125(2), e2019JF005369. <https://doi.org/10.1029/2019JF005369>
- Roelofs, L., Nota, E., Flipsen, T., Colucci, P., & De Haas, T. (2023). How bed composition affects erosion by debris flows—An experimental assessment. *Geophysical Research Letters*, 50(14), e2023GL103294. <https://doi.org/10.1029/2023gl103294>
- Santi, P., Higgins, J., Cannon, S., & Gartner, J. (2008). Sources of debris flow material in burned areas. *Geomorphology*, 96(3–4), 310–321. <https://doi.org/10.1016/j.geomorph.2007.02.022>
- Schürch, P., Densmore, A. L., Rosser, N. J., & McArdell, B. W. (2011). Dynamic controls on erosion and deposition on debris-flow fans. *Geology*, 39(9), 827–830. <https://doi.org/10.1130/g32103.1>

- Shi, Z., Zheng, H., Yu, S., Peng, M., & Jiang, T. (2018). Application of CFD-DEM to investigate seepage characteristics of landslide dam materials. *Computers and Geotechnics*, *101*, 23–33. <https://doi.org/10.1016/j.compgeo.2018.04.020>
- Simoni, A., Bernard, M., Berti, M., Boreggio, M., Lanzoni, S., Stancanelli, L., & Gregoretti, C. (2020). Runoff-generated debris flows: Observation of initiation conditions and erosion–deposition dynamics along the channel at Cancia (eastern Italian Alps). *Earth Surface Processes and Landforms*, *45*(14), 3556–3571. <https://doi.org/10.1002/esp.4981>
- Song, P., & Choi, C. (2021). Revealing the importance of capillary and collisional stresses on soil bed erosion induced by debris flows. *Journal of Geophysical Research: Earth Surface*, *126*(5), e2020JF005930. <https://doi.org/10.1029/2020jef005930>
- Sovilla, B., Burlando, P., & Bartelt, P. (2006). Field experiments and numerical modeling of mass entrainment in snow avalanches. *Journal of Geophysical Research*, *111*(F3), F03007. <https://doi.org/10.1029/2005jf000391>
- Stock, J., & Dietrich, W. (2003). Valley incision by debris flows: Evidence of a topographic signature. *Water Resources Research*, *39*(4), 1089. <https://doi.org/10.1029/2001wr001057>
- Stoffel, M., Tiranti, D., & Huggel, C. (2014). Climate change impacts on mass movements — Case studies from the European Alps. *Science of the Total Environment*, *493*, 1255–1266. <https://doi.org/10.1016/j.scitotenv.2014.02.102>
- Takahashi, T. (2007). Debris flows: Mechanics, prediction and countermeasures. *Proc. Monogr. Eng. Water Earth Sci., Taylor and Francis*.
- Theule, J., Liébault, F., Laigle, D., Loye, A., & Jaboyedoff, M. (2015). Channel scour and fill by debris flows and bedload transport. *Geomorphology*, *243*, 92–105. <https://doi.org/10.1016/j.geomorph.2015.05.003>
- Tiranti, D., Bonetto, S., & Mandrone, G. (2008). Quantitative basin characterisation to refine debris-flow triggering criteria and processes: An example from the Italian western Alps. *Landslides*, *5*(1), 45–57. <https://doi.org/10.1007/s10346-007-0101-4>
- Wang, G., Sassa, K., & Fukuoka, H. (2003). Downslope volume enlargement of a debris slide–debris flow in the 1999 Hiroshima, Japan, rainstorm. *Engineering Geology*, *69*(3–4), 309–330. [https://doi.org/10.1016/s0013-7952\(02\)00289-2](https://doi.org/10.1016/s0013-7952(02)00289-2)
- Wheaton, J., Brasington, J., Darby, S., & Sear, D. (2010). Accounting for uncertainty in DEMs from repeat topographic surveys: Improved sediment budgets. *Earth Surface Processes and Landforms*, *35*(2), 136–156. <https://doi.org/10.1002/esp.1886>
- Zheng, H., Shi, Z., De Haas, T., Shen, D., Hanley, K., & Li, B. (2022). Characteristics of the impact pressure of debris flows. *Journal of Geophysical Research: Earth Surface*, *127*(3), e2021JF006488. <https://doi.org/10.1029/2021jef006488>
- Zheng, H., Shi, Z., Hanley, K., Zhou, Y., & Hu, X. (2023). Pore pressure evolution in bed sediment overridden by debris flow: A general formulation. *Earth Surface Processes and Landforms*, *48*(6), 1188–1201. <https://doi.org/10.1002/esp.5542>
- Zheng, H., Shi, Z., Yu, S., Fan, X., Hanley, K., & Feng, S. (2021). Erosion mechanisms of debris flow on the sediment bed. *Water Resources Research*, *57*(12), WR030707. <https://doi.org/10.1029/2021wr030707>